PCCP

Accepted Manuscript

ROYAL SOCIETY OF CHEMISTRY

www.rsc.org/pccp

Remarkable Conformational Flexibility of Aqueous 18-Crown-6 and its Strontium(II) Complex - Ab initio Molecular Dynamics Simulations

*Lorenz R. Canaval, Saprizal Hadisaputra and Thomas S. Hofer**

Theoretical Chemistry Division,
Institute of General, Inorganic and Theoretical Chemistry
University of Innsbruck, Innrain 80-82, A-6020 Innsbruck, Austria
E-Mail: T.Hofer@uibk.ac.at
Tel.: +43-512-507-57102
Fax: +43-512-507-57199

March 31, 2015

*Corresponding author

Textual Abstract: Ab initio QMCF-MD simulations of aqueous 18-crown-6 (18C6) and strontium(II)–18-crown-6 (18C6-Sr) were performed to gather insight into their hydration properties. Strongly different characteristics were found for the two solutes in terms of structure and dynamics such as H-bonding. They, however, have in common that their backbone shows high flexibility in aqueous medium, adopting structures significantly differing form idealized gas phase geometries. In particular, planar oxyethylene units stable on the picosecond range occurred in 18C6, while the strontium complex readily exhibits a bent structure. Detailed analysis of this high flexibility was done via two dimensional root mean square deviation plots as well as the evolution of dihedral angles and angles within the simulation trajectory. The vibrational spectra obtained from the QMCF-MD simulations are in excellent agreement with experimental data and show a pronounced blueshift upon complexation of the strontium(II) ion in 18C6.

Graphical Abstract:

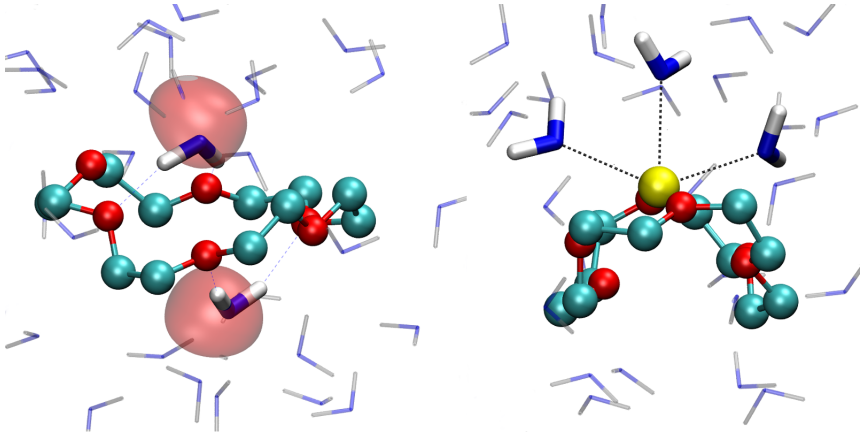

Table of Contents Entry: QM/MM simulations of 18-crown-6 and its strontium(II) complex indicate vivid backbone flexibility in aqueous medium.

1 Introduction

In this work structural and dynamical properties of the hydration of 18-crown-6 (18C6, 1,4,7,10,13,16-hexaoxacyclooctadecane) and its strontium(II) complex (18C6-Sr) are investigated employing ab initio quantum mechanical molecular mechanical molecular dynamics (QM/MM-MD) simulations. Since their discovery in 1967 cyclic polyethers called 'crown ethers'[1] have been studied extensively due to their wide-spread applications in chemistry and their ability to selectively bind both metal and organic cations. Crown ether compounds are tested in antitumor research,[2] the treatment of nuclear waste,[3] used as catalysis agents[4] and have the ability to influence chemical reactions.[5] Recently crown ethers were found to dramatically modify protein surface behavior.[6]

Crown ethers are large systems on the scale of quantum mechanical calculations, which is why previous studies often investigated their properties in the gas phase or using implicit solvent, whereas simulations in aqueous medium artificially kept the structure rigid using idealized, rigid gas phase geometries.[7–9] High symmetry structures of 18C6 and its complexes are employed, with typical C–O distances of 1.42 Å, C–C distances of 1.51 Å, C–O–C angles of 112 degree, and O–C–C–O dihedral angles of 76 degrees (18C6 at MP2/6-31+G* level of theory)[10] (compare figure 1).

18C6's hydration structure was investigated using molecular dynamics of its D_{3d} conformer applying a united atom approximation for CH_2, where it was reported that on both sides of the crown ether's plane a distinct water molecule was translationally fixed by preferably two H-bonds.[7] Two bridging

water molecules bound to the crown ether were observed in a semiempirical QM/MM study using a rigid 18C6 model along with rigid SPC/E water.[8] Krongsuk *et al.* conducted a Monte Carlo (MC) study based on ab initio derived potentials of 18C6 solvated in 500 water molecules, fixing the ether's geometry to the D_{3d} gas phase structure and using rigid solvent.[9] The simulation at hand indicates an average coordination number of one, but it was found that the first hydration shell can also accommodate two water molecules, one on either side of the macrocycle's plane, forming mobile H-bonds with 18C6.

Agents based on 18-crown-6 are reported to be among the most effective for strontium extraction in nuclear waste.[11,12] These compounds also exhibit strong affinity to bind other divalent ions such as mercury, barium and lead, while they have been shown to have almost no tendency to bind calcium(II) and a range of monovalent ions such as potassium.[13] Radioactive strontium(II) is highly abundant in nuclear waste and is a major part of the environmental pollution by nuclear accidents.[14] At the same time its chemical properties are very similar to calcium(II), which is why the human body readily incorporates strontium(II) into bone tissue. This enrichment may lead to serious diseases such as bone cancer and leukemia.[15,16] Due this importance, the 18C6-Sr complex was chosen as a model system to be compared to the free 18C6 in aqueous medium. Experimentally, Gámez *et al.* reported that the most stable conformer for the 18C6-Sr adduct is not planar in a laser infrared multiple photon dissociation study, but the ion is bound in an open conformation.[17]

The present work does not impose any restriction to the crown ethers

conformational degrees of freedom, i.e. all C–C and C–O bonds as well as all associated angles and dihedral degrees of freedom of the macrocycle may evolve without any constraint. Finite temperature and a chemical environment providing H-bond partners enable the crown ether to access a wide range of its conformational space, which was found to be of critical importance in aqueous medium. This is especially true upon incorporation of solutes such as strontium(II), where some coordination sites are provided by the ether, while others are occupied by water ligands displaying exchange dynamics on the picosecond scale. The notable difference between idealized gas phase properties and those observed in aqueous solution promised to significantly contribute to the knowledge of the behavior in solution by conducting ab initio simulations with minimal constrains. In the following sections the QM method is outlined and results obtained from the simulations of 18C6 and 18C6-Sr in aqueous solution are presented.

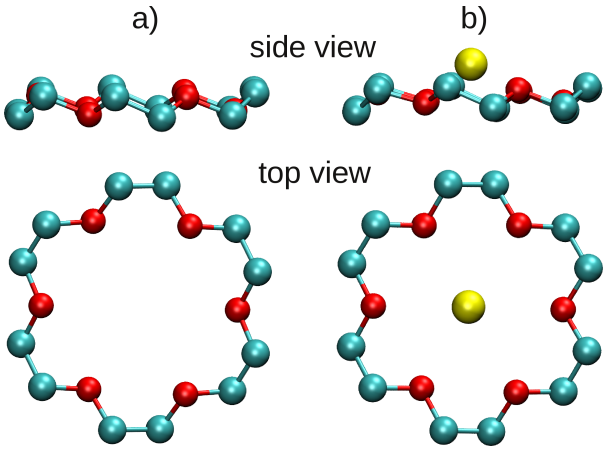

Figure 1: Illustrations of typical high symmetry structures of a) 18C6 and b) 18C6-Sr as obtained from geometry optimizations in vacuum or implicit solvent.

2 Methods

2.1 QMCF-MD approach

In this study the well established *ab initio* quantum mechanical charge-field molecular dynamics (QMCF-MD) approach[18–21] has been employed as it already yielded valuable insights into the hydration properties of numerous of ions,[22,23] inorganic complexes[24–26] and host-guest complexes such as magnesium(II)-porphyrin.[27]

The QMCF-MD framework bases on standard QM/MM approaches, but does not require knowledge of non-Coulombic solute–solvent potentials. This is achieved by enlarging the QM region and separating it into a core zone, containing at least the solute species, and a layer zone. For particles in the layer zone, non-Coulombic interactions with atoms in the MM region have to be evaluated. A quantum mechanical treatment intrinsically includes polarization, charge-transfer and many-body effects, which guarantees a high degree of accuracy compared to non-polarizable simulation techniques. To ensure a realistic embedding of the entire QM region, all point charges of the classically treated region are accounted for via a perturbation term of the Hamiltonian of the QM calculations. Quantum mechanically derived partial charges are evaluated in every MD step and used to calculate the long range Coulombic interactions. Further details of the QMCF-MD methodology have been published elsewhere.[18–21]

2.2 Simulation protocol

Ab initio QMCF-MD simulations were carried out for both the hydrated 18C6 molecule and the hydrated $[18C6\text{-}Sr]^{2+}$ complex. Besides these solute species the cubic boxes (side lengths of 44.9 Å) contained 3000 water molecules. Periodic boundary conditions and the minimal image convention were applied. For the integration of the equations of motion the Velocity–Verlet[28,29] algorithm was employed with a time step to 2 fs. The Berendsen theromstat[30] using a relaxation time of 0.1 ps was applied to keep the temperature at 298.15 K. Beyond the Coulombic cutoff distance of 15 Å, the reaction field method[31] was employed to treat long-range electrostatic interactions ($\epsilon = 78.0$). The M-RATTLE algorithm[32,33] was used to constrain the geometry of the water molecules (1.00 Å, 109.47°), whereas the length of the crown ethers' H-bonds were constrained using the RATTLE approach[32,34,35] (1.093 Å). The atomic partial charges of water in the MM region were chosen according to the SPC/E water model,[36,37] and the fluctuating atomic charges in the QM regions were evaluated by Mulliken population analysis[38,39] in every MD step. Classical MD simulations with a total simulation time of 150 ps for each system including heating steps were conducted prior to the QMCF-MD runs for a proper equilibration. After re-equilibration of 3 ps sampling was performed for 97 ps. For the *ab initio* simulations the geometric center of the crown ethers' carbon and oxygen atoms served as the centroid (CEN) of the QM area. The core zone was chosen to have a diameter of 0.2 Å to include no particles in the 18C6 simulation, but the strontium ion in the 18C6-Sr simulation. The layer zone was defined with a diameter

of 15.2 Å including a smoothing region of 0.2 Å enabling a smooth transition of molecules between the MM and QM region. As a result, the QM area was populated with the solute molecule(s) plus 36 (18C6) and 40 (18C6-Sr) water molecules in average. The Hartree-Fock level of theory was chosen along with the well established double-ζ polarization basis sets[40] for hydrogen, carbon and oxygen. Similar conditions have already been employed successfully for the investigation of other metal-organic complexes.[25,27,41] For the strontium(II) ion the Stuttgart RSC 1997 basis set including a quasi relativistic effective core potential accounting for 28 inner electrons[42] was obtained from the EMSL database.[43,44] All quantum chemical calculations were carried out with the Turbomole 6.4[45–47] package.

2.3 Analyzed Properties

The structure and picosecond dynamics of the solute species were analyzed via distributions of water oxygen (O_w) and hydrogen (H_w). Radial distribution functions (RDF) of O_w and H_w were evaluated with respect to the center of the QM region (CEN and Sr(II), respectively) and the oxygen atoms of the crown ethers (O_{crown}). Visual analysis of the trajectory has been done using the *Visual Molecular Dynamics* (VMD) package.[48]

The lifetime and structural relaxation of H-bonds accepted by the crown ethers' oxygen atoms were analyzed employing the continuous hydrogen bond time correlation S(t) (equation 1) and the intermittent hydrogen bond time correlation function C(t) (equation 2) as described in literature[49] and applied in previous investigations of hydration properties of molecules[50] and metal-

organic complexes.[26,27]

$$S(t) = \frac{\langle h(0)H(t)\rangle}{\langle h\rangle} \tag{1}$$

$$C(t) = \frac{\langle h(0)h(t)\rangle}{\langle h\rangle} \tag{2}$$

$H(t)$ and $h(t)$ refer to two defined hydrogen bond population variables.[49] The $h(t)$ variable is 1 if a H-bond between a specific donor–acceptor pair is detected at time t, otherwise it's zero. In contrast, $H(t)$ amounts to 1 only if an H-bond continuously exists from time 0 to time t. A hydrogen bond exists if the distance between the two involved oxygen atoms is less than 3.25 Å and the H-bond angle is less than 35°, which is the recommended and widely accepted criterion.[49] Both time correlation functions were fitted to the double-exponential expression shown in equation 3, τ_l and τ_s corresponding to the long and short contribution of the correlation function, respectively. The long contribution yields a handy number to gain insight into the H-bond lifetime conditions, whereas the short one has less impact for our applications.

$$y = a \cdot e^{-t/\tau_l} + (1-a) \cdot e^{-t/\tau_s} \tag{3}$$

3 Results and Discussion

3.1 Structure

Strongly differing hydration structures were observed for 18C6 and 18C6-Sr. The CEN–O_w, CEN–H_w, Sr–O_w and Sr–H_w radial distribution functions including the corresponding integration information are presented in figure 2. For the 18C6 system the first peak maxima are located at 1.80 (CEN–H_w) and 2.10 Å (CEN–O_w). According to these values, the water's hydrogen atoms point towards the crown ether moiety, indicating the formation of H-bonds to the crow ether's oxygen atoms. The integration information reveals that in average one water molecule is located within this region. A broad second peak is centered at 4.0 (CEN–H_w) and 4.6 Å (CEN–O_w). The existence of a non-zero valley between the first and second CEN–H_w and CEN–O_w peaks indicates vivid exchange activities within these regions. The entire crown ether molecule is covered by a hydration shell, which can be concluded from the pronounced peak at 7.45 Å(CEN–O_w). Beyond this solvation structure, the water distribution is homogenous. A large hydration pattern of the 18C6 molecule at low concentrations is underlined by results of volumetric[51] and compressibility experiments.[51–53] The average coordination number of one for 18C6 is fair agreement with previous simulation studies, which reported a value of two.[7–9] Since 18C6 was artificially constrained to a gas phase geometry in the previous studies,[7–9] this deviation can be explained by the conformational flexibility having a strong impact on the the coordination environment.

For the $[18C6\text{-}Sr]^{2+}$ complex the first shell's peak maxima are found at

2.68 (Sr–O_w) and 3.30 Å (Sr–H_w). In contrast to 18C6, the water molecules are differently oriented: the water's oxygen atoms are coordinating to the positively charged Sr(II) ion, in agreement with the structure of the strontium(II) ion in pure water.[23] The ion is coordinated by 2 (23%), 3 (65%) or 4 (12%) water molecules (average 2.9, see figure 4c), being in constant exchange, which is indicated by a non-zero valley ranging from the first to the second Sr–O_w (5.25 Å) maximum. Binding the ion, the crown ether contributes six coordinating oxygen atoms, which yields a total coordination number of 8-10. The findings are in excellent agreement with a previous QM/MM study on strontium(II) in aqueous solution, where a predominant coordination of 9 water ligands (90%) and an almost equally small probability of a 8- and 10-fold (5%) arrangement is reported.[23] Chekholv observed a coordination of three water molecules for crystals of the hydrated complex of strontium with 18C6 using X-ray diffraction analysis.[54] Furthermore it is interesting to note that the results found are in good agreement with the three- and four fold water coordination found for hydrated complexes of 18C6 with lanthanoide(III) ions such as cerium, neodymium, samarium, europium, gadolinium and terbium,[55] which have similar ionic radii as strontium.

Figure 3 displays the O_{crown}–O_w and O_{crown}–H_w radial distribution functions for 18C6 and 18C6-Sr. Plot 3a shows two distinct peaks for these atoms pairs, indicating that one water molecule points toward each of the crown's oxygen atoms with a distance of approximately 2.1 Å, forming an H-bond O_{crown}–H_w–O_w. The O_{crown}–O_w RDF shows a broad peak at 3.1 Å, which compares well with values of 2.862 to 2.891 Å reported for the crystal structure of a binary hydrate of 18C6.[56] In contrast, almost no H-bonds to bulk

water molecules can be observed upon complexation of strontium(II) during the 100 ps trajectory. This finding is underlined by data presented in figures 4a and b, where the distribution of the number of H-bonds to O_{crown} is displayed. In 18C6, the six O_{crown} atoms readily form one (53%) or (4%) two H-bonds with bulk water, while in 43% of the cases no H-bond was observed. This pattern dramatically changes upon incorporation of the guest ion strontium, where no H-bonding to surrounding water molecules was observed in 94% of the cases, while the probability for one H-bond decreases to 5%. The behavior observed is reasonable as the negatively polarized oxygen atoms of 18C6 are expected to form H-bonds with water molecules. In the $[18C6\text{-}Sr]^{2+}$ complex in contrast, the O_{crown} atoms already coordinate to the strontium(II) ion, which is why they are less subject to form H-bonds. Figures 4a and b display the average values for all O_{crown} atoms in the respective system. A separate analysis for each O_{crown} is included in the supporting information demonstrating that all six atoms have very similar distributions (see figures S.1 and S.2).

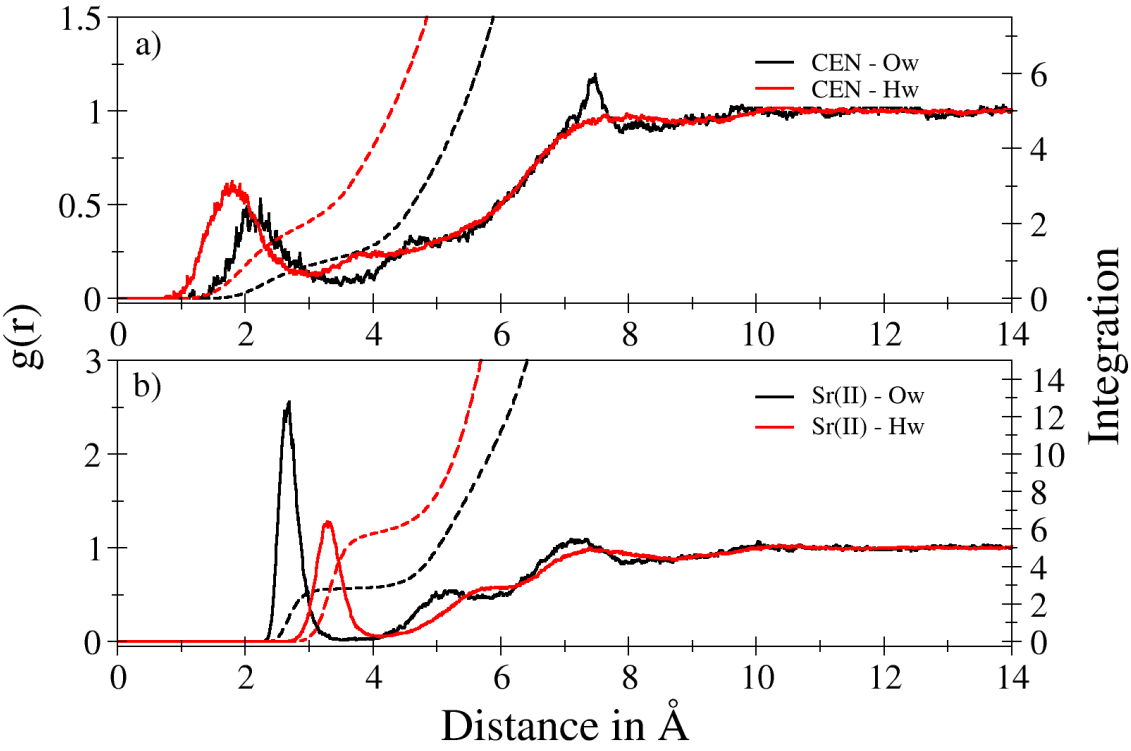

Figure 2: Radial distribution functions (solid) of oxygen (O_w) (black) and hydrogen (H_w) (red) atoms of water plus the corresponding integration curve (dashed) with respect to a) CEN in 18C6 and b) Sr(II) in 18C6-Sr.

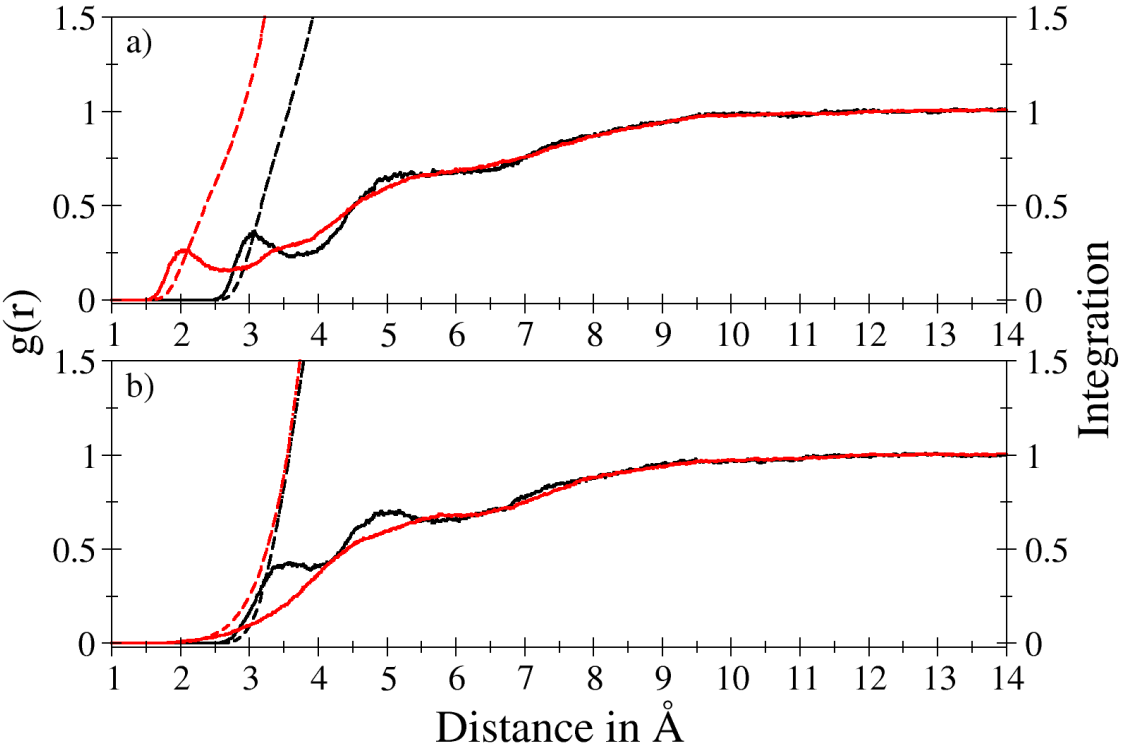

Figure 3: Radial distribution functions (solid) of oxygen (O_w) (black) and hydrogen (H_w) (red) atoms of water plus the corresponding integration curve (dashed) with respect to the six oxygen atoms O_{crown} of the crown ethers for a) 18C6 and b) 18C6-Sr.

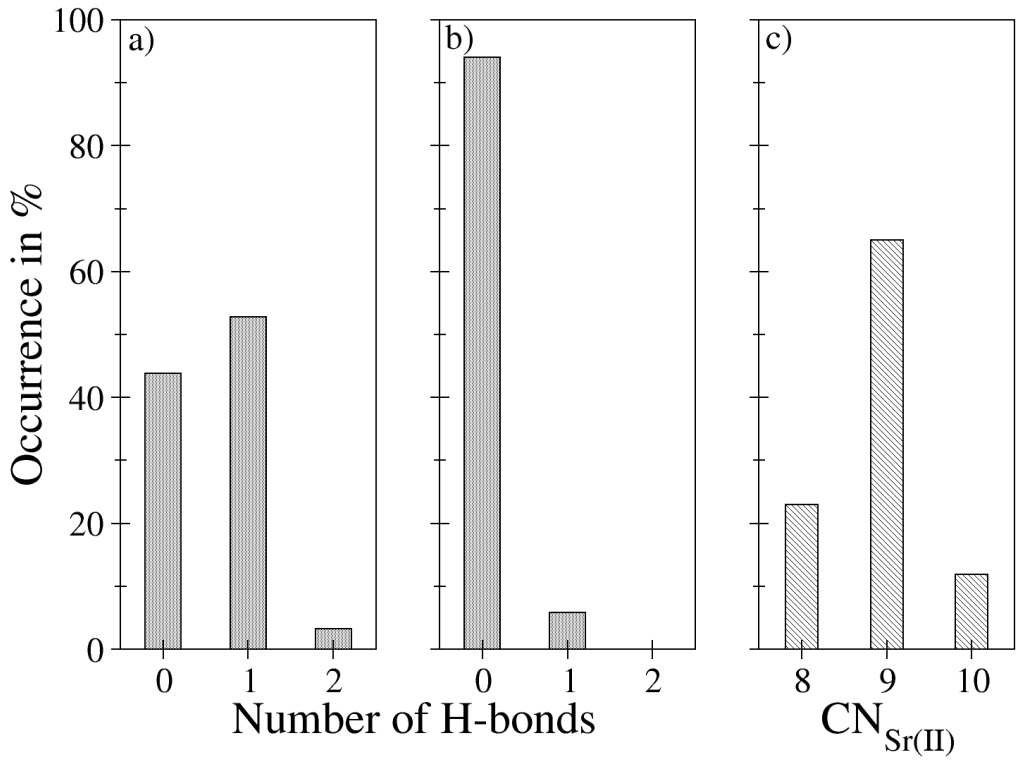

Figure 4: Number of H-bonds from water molecules to O_{crown} for a) 18C6, and b) 18C6 binding strontium(II). Histogram c) presents the total coordination number (CN) of the ion in 18C6-Sr including the six oxygen atoms of the crown moiety plus coordinated water molecules.

3.2 Dynamics

3.2.1 Conformational Flexibility

Classical equilibration after embedding a 18C6 gas phase structure in water yielded a distorted and asymmetric structure after plenty of equilibration time (snapshot 5c). This starting structure for the QMCF-MD run possess four dihedral angles of approximately +70 degree, whereas only two angles have a negative sign, which is in clear contrast to the high symmetry gas phase structure, where alternating values of approximately ±76 degree

are found (see snapshot 1a). Figure 5a depicts the two dimensional root-mean-square deviation (2D-RMSD) of 18C6 for the QMCF-MD simulation, showing three distinct regions with similar structures. Within the first 25 ps of simulation time no dramatic change of the polyether's structure can be observed, although a high degree of conformational flexibility is indicated by a short change of one of the improper torsions at t_2 (snapshot 5d). The second distinct region in the 2D-RMSD plot ranges from 25 to approximately 70 ps simulation time, where vivid changes and inversions of dihedral angles are visible. Conformations with one (t_3, snapshot 5e) and even two (t_4, snapshot 5f) planar oxyethylene moieties are accessible and stable on the picosecond scale. The geometry of 18C6 in the region ranging from 70 to 100 ps is characterized by four positive and two negative improper torsion angles like in the first region, but for different O–C–C–O quadruples. Snapshot 5g illustrates this structure plus two water molecules bridging via H-bonds. It is further interesting to note that no gas phase like structure of 18C6 has been observed within 0.1 ns of simulation time. To conclude, water environment dramatically enhances the crown ether's conformational flexibility by H-bonding to single oxygen atoms, but also by double hydrogen-bonding (bridging) as illustrated in snapshots 5c, d, e and g. Two bridging water molecules H-bonded to the crown ether have already been proposed in the interpretation of experimental near infrared spectral studies to investigate the hydration of 18C6 in aqueous solution,[53] however, for higher concentrations up to 4 M.

Figure 6a depicts the 2D-RMSD of the $[18C6\text{-}Sr]^{2+}$ complex simulation trajectory. Distinct regions are visible, indicating similar conformations of

the 18C6 backbone. Snapshot 6c (t_1) illustrates the rather planar starting geometry with four water molecules coordinated to the ion, which was obtained via a purely classical simulation. Within the first picosecond of simulation time one water is expelled of the coordination sphere of strontium, while the conformation of the crown ether remains planar (t_2, snapshot 6d). Between picosecond 27 and 35, the 2D-RMSD plot indicates a pronounced change in the backbone's conformation with one O–Sr–O angle close to planarity (t_3, snapshot 6e). Such a bent structure allows all six crown ether oxygen atoms to readily fill the ion's coordination sphere as they are not arranged in one single plane, which mimics the coordination in aqueous solution. Two occasions were found where the crown ether plus four water molecules arrange in a way that a highly symmetrical bicapped square antiprismatic coordination polyhedron results (t_5, snapshot 6g). Glendening *et al.* speculated that there are structures of 18C6-Sr of lower symmetry than D_{3d}, which are favored in the gas phase, they were however unable to identify those.[57]

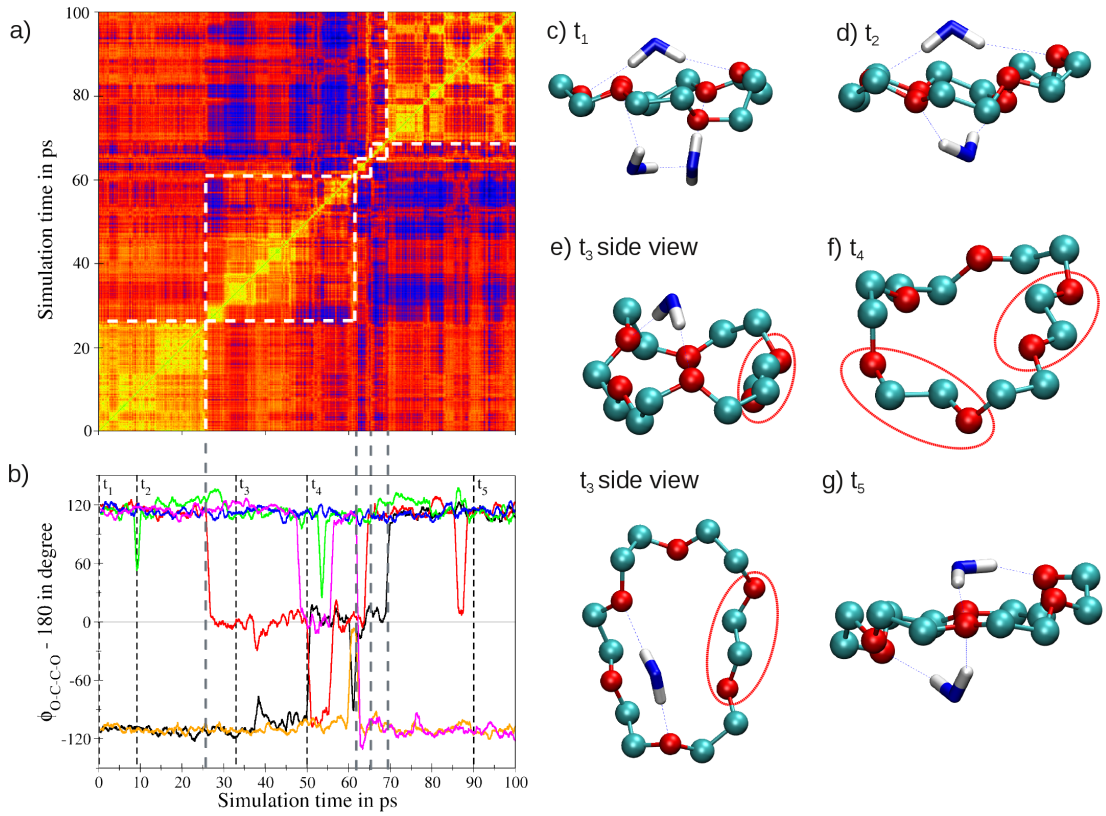

Figure 5: Detailed analysis of the pronounced backbone flexibility of 18C6 in aqueous medium using a) a two dimensional RMSD plot (coloring: green–orange–blue for RMSD values of 0.0, 1.0 and 2.0 Å, respectively) and b) evolution of the six O–C–C–O improper torsions during the simulation time of 100 ps. Snapshots c)-g) illustrate the high degree of distortion of 18C6 including planar oxyethylene units (red ovals) in comparison to the gas phase structure depicted in figure 1a.

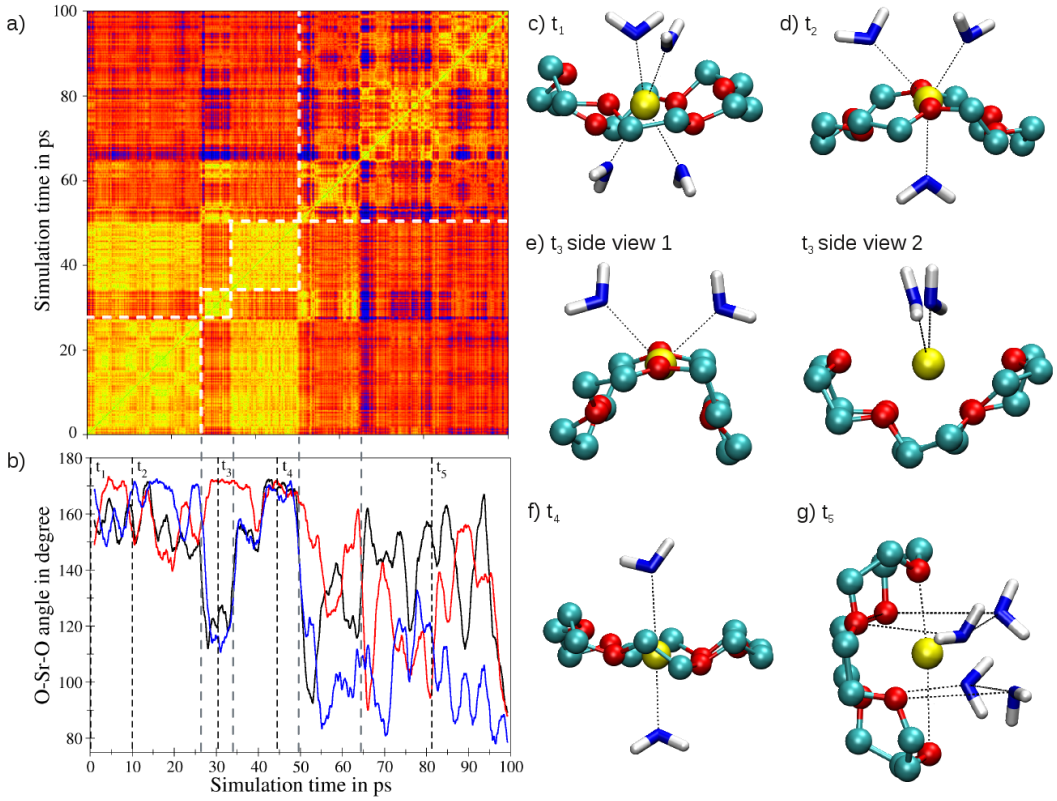

Figure 6: Detailed analysis of the pronounced backbone flexibility of 18C6-Sr in aqueous medium using a) a two dimensional RMSD plot (coloring: green–orange–blue for RMSD values of 0.0, 1.0 and 2.0 Å, respectively) and b) evolution of the three O–Sr–O angles of opposite oxygen atoms during the simulation time of 100 ps. Snapshots c)-g) illustrate the high degree of distortion of 18C6-Sr in comparison to the gas phase structure depicted in figure 1b.

3.2.2 Fluctuation of charges

The fluctuating atomic partial charges derived by Mulliken population analysis were saved in every step of the QMCF-MD simulations and analyzed for the solutes' atoms (see table 1). The oxygen atoms were found to be negatively charged, which underlines the fact that they play a crucial role in H-bonding to water molecules. The strontium complex shows a charge-

transfer from the ion to the oxygen atoms lowering the charge from −0.51 (18C6) to −0.58 a.u. (strontium complex), which also significantly lowers the ion's formal charge from +2 to +1.50 a.u. It is worth noting that upon incorporation of strontium, the partial charges of carbon and hydrogen are slightly more positive. Similar results were reported for the hydration properties of prophyrin and its magnesium(II) adduct.[27] In the case of the empty crown ether the charge transfer to the environment is negligible (−0.06 a.u.), however, it changes by 0.18 a.u. upon binding the ion. This implies that approximately 0.2 a.u. of electron density are transferred from the crown ether moiety to the ion, while another 0.3 a.u. originate from the surrounding water molecules. The occurrence of such charge transfer effects underlines the importance of an accurate quantum mechanical treatment of the solute plus and the surrounding solvent molecules, as such effects are difficult to accurately describe using purely classical simulation approaches.

Table 1: Average partial atomic charges in a.u. obtained via Mulliken population analysis in very MD step for 18C6 and 18C6-Sr. $\Sigma_{crown-atoms}$ corresponds to the total charge of the crown ether molecule excluding the ion.

Atoms	18C6	18C6-Sr
Sr(II)	–	$+1.50 \pm 0.02$
O	-0.51 ± 0.02	-0.58 ± 0.02
C	$+0.05 \pm 0.01$	$+0.06 \pm 0.01$
H	$+0.10 \pm 0.00$	$+0.12 \pm 0.00$
$\Sigma_{crown-atoms}$	−0.06	+0.12

3.2.3 Hydrogen bonding and mean residence times

The results of the H-bond analysis are summarized in table 2 and underline the finding from RDF (figure 3) and CND (figure 4) analysis that H-bonding to crown ether oxygen atoms is significantly decreased upon incorporation of the ion. While the mean C(t) value amounts to 1.3 ps in 18C6, it dramatically changes to 0.4 ps for the strontium complex indicating that the latter species allows fewer H-bonds to bulk water molecules and at the same the average lifetime of the few H-bonds observed is shortened.

The mean residence time of the water ligands coordinated to strontium(II) amounts to 9.5 ps, which significantly differs from the corresponding value of bulk water, being 1.6 ps.[58] The MRT indicates a five times faster ligand exchange rate at the strontium(II) ion bound to 18C6 compared to the free ion in aqueous solution, where a MRT of 45 ps was found.[23] While every second exchange attempt lasts longer than 0.5 ps for the present system, a sustainability coefficient of 0.22 was reported for the free ion, meaning that every 4th to 5th exchange is considered successful.[23] During the simulation time of 100 ps, a total of 31 ligand exchange events were observed, demonstrating that the ion–water interaction seems to be significantly lowered upon complexation by 18C6. This is in contrast to conclusions drawn from a comparative study on the hydration properties of porphyrin and its magnesium(II) complex, where enhanced stability for the coordination of the only water ligand was reported.

Table 2: Computed C(t) and S(t) correlation functions. τ values are given in ps.

Atom	18C6		18C6-Sr	
	C(t)	S(t)	C(t)	S(t)
	τ_l	τ_l	τ_l	τ_l
O-07	1.28	0.209	0.797	0.018
O-14	1.25	0.156	0.222	0.043
O-21	2.19	0.211	0.132	0.113
O-28	1.16	0.248	0.162	0.098
O-35	1.30	0.136	0.053	0.038
O-42	1.24	0.156	0.513	0.054
O-all	1.30	0.187	0.414	0.070

3.2.4 Power spectra via Fourier transformed velocity autocorrelation functions

Figure 7 depicts the power spectra of the free crown ether and its strontium complex as obtained via Fourier transformed VACFs from the QMCF-MD simulations. As bonds involving hydrogen have been kept rigid, the corresponding vibrational modes could not be determined in this work. The frequencies have been scaled by a factor of 0.9046 as proposed for calculations on the Hartree-Fock level of theory employing DZP basis sets.[59] This yields results in very good agreement with Raman shifts for 18C6 in aqueous solution reported by Ozutsumi *et al.*[60] and also a very good overall agreement with infrared (IR) and Raman values reported for uncomplexed 18C6.[61] The spectrum of the strontium coordinated 18C6 is shifted to higher values, which confirms the strong interaction of the ether and the earth alkali ion. It is worth noting that such a blueshift has also been observed both experimentally[62] and theoretically[27] in works investigating the hydration of porphyrin and its divalent metal complexes. Experimental work employing

laser infrared multiple photon dissociation (IRMPD) spectroscopy yielded two differentiated bands at 943 and 1057 $^{-1}$ for the strontium complex, corresponding to C–C and C–O stretching modes.[17] The overall good agreement confirms the general applicability of the simulation approach since frequencies depend on the second derivatives of the energy with respect to the nuclear coordinates, thus being a sensitive probe of the accuracy of the simulations. A detailed comparison of the observed frequencies is presented in table 3 and figure 7.

Table 3: Comparison of experimental absorption maxima with the values derived from the QMCF-MD simulations via Fourier transformed VACFs (scaled by 0.9046[59]) in cm^{-1}.

18C6			18C6-Sr	
QMCF-MD	Exp. Raman[60]	Exp. Raman / IR[61]	QMCF-MD	Exp. IRMPD[17]
288	282	274 / –	291	
518	549	525 / 538	567	
811, 824, 846	815, 836, 860	825, 836, 868 / 828, 835, 861	854	
950	–	939 / 945	968	943
1046	1046,1073	1049 / 1043	1080	1057
1149	1139	1159 / 1159	1149	
1289	1247	1276 / 1274	1374	
1495	1455, 1475	1495 / 1496	1647	

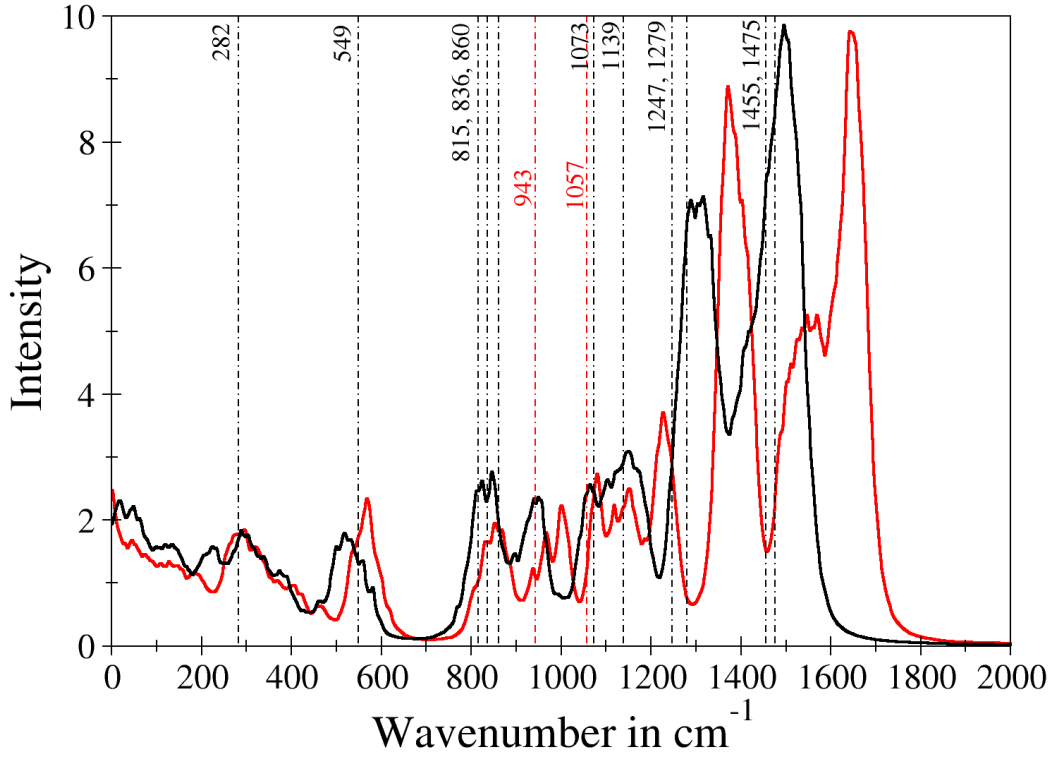

Figure 7: Power spectra obtained from the QMCF-MD simulations for 18C6 (black solid) and its strontium(II) complex (red solid) in aqueous solution. Experimental results are presented as dashed lines along with the corresponding values for comparison (18C6: black dashed, 18C6-Sr: red dashed).[17,60]

4 Conclusion

Two QMCF-MD simulations were carried out to investigate the structure and picosecond dynamics of 18-crown-6 and its strontium(II) in dilute aqueous medium. In contrast to the gas phase and crystal structures, the hydrated species were found to have considerable conformational flexibility, allowing vivid interaction with the solvent. 18C6 binds up to two water molecules on each side of the crown ether's plane via one H-bond or in a bridging mode via two H-bonds. However, due to conformational flexibility in average only one

water molecule is coordinated to 18C6 as opposed to previous studies were the crown moiety was modeled in a restrained, idealized gas phase geometry. In addition, the crown ether's oxygen atoms readily form one H-bond to the bulk solvent. In the strontium complex two to four water molecules under constant exchange are coordinated to the crown ether moiety, which can adopt a bent structure and does not form any H-bonds to bulk water. The simulations yielded valuable insight into the strong conformational flexibility of both 18C6 backbones, allowing planar dihedrals and strongly distorted structures. All properties derived from the QM/MM simulations are in excellent agreement with experimental data were available, which is especially true for the vibrational analysis, underlining the overall excellent accuracy of the calculations carried out.

Acknowledgment Financial support from a PhD grant of the Leopold-Franzens-University of Innsbruck (Rector Univ.Prof. Dr. Dr.hc.mult. Tilmann D. Märk) for Lorenz R. Canaval is gratefully acknowledged. This work was supported by the Austrian Ministry of Science BMWF UniInfrastruktur-programm as part of the Research Focal Point Scientific Computing at the University of Innsbruck.

References

[1] Pedersen, C. J. *J. Am. Chem. Soc.* **1967**, *89*, 7017–7036.

[2] Marjanovic, M.; Kralj, M.; Supek, F.; Frkanec, L.; Piantanida, I.; Šmuc, T.; Tušek-Bozic, L. *J. Med. Chem.* **2007**, *50*, 1007–1018.

[3] Horwitz, E. P.; Dietz, M. L.; Fisher, D. E. *Anal. Chem.* **1991**, *63*, 522–525.

[4] Childs, M. E.; Weber, W. P. *J. Org. Chem.* **1976**, *41*, 3486–3487.

[5] Durst, H. D. *Tetrahedron Lett.* **1974**, *15*, 2421–2424.

[6] Lee, C.-C.; Maestre-Reyna, M.; Hsu, K.-C.; Wang, H.-C.; Liu, C.-I.; Jeng, W.-Y.; Lin, L.-L.; Wood, R.; Chou, C.-C.; Yang, J.-M. *Angew. Chem. Int. Ed.* **2014**, *53*, 13054–13058.

[7] Kowall, T.; Geiger, A. *J. Phys. Chem.* **1994**, *98*, 6216–6224.

[8] Thompson, M. A. *J. Phys. Chem.* **1995**, *99*, 4794–4804.

[9] Krongsuk, S.; Kerdcharoen, T.; Hannongbua, S. *J. Phys. Chem. B* **2003**, *107*, 4175–4181.

[10] Al-Jallal, N.; Al-Kahtani, A.; El-Azhary, A. *J. Phys. Chem. A* **2005**, *109*, 3694–3703.

[11] Xu, C.; Wang, J.; Chen, J. *Solvent Extr. Ion Exch.* **2012**, *30*, 623–650.

[12] Horwitz, E.; Dietz, M. L.; Fisher, D. E. *Solvent Extr. Ion Exch.* **1990**, *8*, 557–572.

[13] Davis, F.; Higson, S. *Macrocycles: Construction, Chemistry and Nanotechnology Applications*; Wiley, 2011.

[14] Ojovan, M.; Lee, W. *An Introduction to Nuclear Waste Immobilisation*; Elsevier Science, 2013.

[15] Mangano, J. J.; Sherman, J. D. *Int. J. Health. Serv.* **2011**, *41*, 137–158.

[16] Froidevaux, P.; Bochud, F.; Haldimann, M. *Long-Term Effects of Exposure to Low-Levels of Radioactivity: a Retrospective Study of 239Pu and 90Sr from Nuclear Bomb Tests on the Swiss Population*; INTECH Open Access Publisher, 2011.

[17] Gámez, F.; Hurtado, P.; Martínez-Haya, B.; Berden, G.; Oomens, J. *Int. J. Mass Spectrom.* **2011**, *308*, 217–224.

[18] Rode, B. M.; Hofer, T. S.; Randolf, B. R.; Schwenk, C. F.; Xenides, D.; Vchirawongkwin, V. *Theor. Chem. Acc.* **2006**, *115*, 77–85.

[19] Hofer, T.; Pribil, A.; Randolf, B.; Rode, B. *Adv. Quantum Chem.* **2010**, *59*, 213–246.

[20] Hofer, T. S.; Rode, B. M.; Pribil, A. B.; Randolf, B. R. *Adv. Inorg. Chem.* **2010**, *62*, 143–175.

[21] Weiss, A. K.; Hofer, T. S. *RSC Adv.* **2013**, *3*, 1606–1635.

[22] Hofer, T. S.; Weiss, A. K.; Randolf, B. R.; Rode, B. M. *Chem. Phys. Lett.* **2011**, *512*, 139–145.

[23] Hofer, T. S.; Randolf, B. R.; Rode, B. M. *J. Phys. Chem. B* **2006**, *110*, 20409–20417.

[24] Tirler, A. O.; Weiss, A. K.; Hofer, T. S. *J. Phys. Chem. B* **2013**, *117*, 16174–16187.

[25] Lutz, O. M.; Messner, C. B.; Hofer, T. S.; Glatzle, M.; Huck, C. W.; Bonn, G. K.; Rode, B. M. *J. Phys. Chem. Lett.* **2013**, *4*, 1502–1506.

[26] Bhattacharjee, A.; Weiss, A. K.; Artero, V.; Field, M. J.; Hofer, T. S. *J. Phys. Chem. B* **2014**, *118*, 5551–5561.

[27] Moin, S. T.; Hofer, T. S. *Mol. BioSyst.* **2014**, *10*, 117–127.

[28] Verlet, L. *Phys. Rev.* **1967**, *159*, 98.

[29] Swope, W. C.; Andersen, H. C.; Berens, P. H.; Wilson, K. R. *J. Chem. Phys.* **1982**, *76*, 637–649.

[30] Berendsen, H. J.; Postma, J. P. M.; van Gunsteren, W. F.; DiNola, A.; Haak, J. *J. Chem. Phys.* **1984**, *81*, 3684–3690.

[31] Adams, D. J.; Adams, E. M.; Hills, G. J. *Mol. Phys.* **1979**, *38*, 387–400.

[32] Horn, H. W.; Swope, W. C.; Pitera, J. W.; Madura, J. D.; Dick, T. J.; Hura, G. L.; Head-Gordon, T. *J. Chem. Phys.* **2004**, *120*, 9665.

[33] Kräutler, V.; van Gunsteren, W. F.; Hünenberger, P. H. *J. Comput. Chem.* **2001**, *22*, 501–508.

[34] Andersen, H. C. *J. Comput. Phys.* **1983**, *52*, 24–34.

[35] Ryckaert, J.-P.; Ciccotti, G.; Berendsen, H. J. *J. Comput. Phys.* **1977**, *23*, 327–341.

[36] Berendsen, H.; Grigera, J.; Straatsma, T. *J. Phys. Chem.* **1987**, *91*, 6269–6271.

[37] Chatterjee, S.; Debenedetti, P. G.; Stillinger, F. H.; Lynden-Bell, R. M. *J. Chem. Phys.* **2008**, *128*, 124511.

[38] Mulliken, R. S. *J. Chem. Phys.* **1955**, *23*, 1833–1840.

[39] Mulliken, R. S. *J. Chem. Phys.* **1955**, *23*, 1841–1846.

[40] Dunning Jr, T. H.; Hay, P. J. *Methods of electronic structure theory*; Springer, 1977; Vol. 2; pp 1–27.

[41] Messner, C. B.; Lutz, O. M.; Rainer, M.; Huck, C. W.; Hofer, T. S.; Rode, B. M.; Bonn, G. K. *J. Phys. Chem. B* **2014**, *118*, 12232–12238.

[42] Kaupp, M.; Schleyer, P. v. R.; Stoll, H.; Preuss, H. *J. Chem. Phys.* **1991**, *94*, 1360.

[43] Feller, D. *J. Comp. Chem.* **1996**, *17*, 1571–1586.

[44] Schuchardt, K. L.; Didier, B. T.; Elsethagen, T.; Sun, L.; Gurumoorthi, V.; Chase, J.; Li, J.; Windus, T. L. *J. Chem. Inf. Model.* **2007**, *47*, 1045–1052.

[45] TURBOMOLE V6.4 2012, a development of University of Karlsruhe and Forschungszentrum Karlsruhe GmbH, 1989-2007, TURBOMOLE

GmbH, since 2007; available from
`http://www.turbomole.com`.

[46] Ahlrichs, R.; Bar, M.; Häser, M.; Horn, H.; Kolmel, C. *Chem. Phys. Lett.* **1989**, *162*, 165–169.

[47] Häser, M.; Ahlrichs, R. *J. Comput. Chem.* **1989**, *10*, 104–111.

[48] Humphrey, W.; Dalke, A.; Schulten, K. *J. Mol. Graphics* **1996**, *14*, 33–38.

[49] Chanda, J.; Chakraborty, S.; Bandyopadhyay, S. *J. Phys. Chem. B* **2006**, *110*, 3791–3797.

[50] Weiss, A. K.; Hofer, T. S.; Randolf, B. R.; Rode, B. M. *Phys. Chem. Chem. Phys.* **2012**, *14*, 7012–7027.

[51] Patil, K.; Pawar, R.; Gokavi, G. *J. Mol. Liq.* **1998**, *75*, 143–148.

[52] Miyazaki, Y.; Matsuura, H. *Bull. Chem. Soc. Jpn.* **1991**, *64*, 288–290.

[53] Patil, K.; Pawar, R. *J. Phys. Chem. B* **1999**, *103*, 2256–2261.

[54] Chekhlov, A. *Russ. J. Inorg. Chem.* **2007**, *52*, 1918–1924.

[55] Misra, P.; Koner, R.; Nayak, M.; Mohanta, S.; Low, J. N.; Ferguson, G.; Glidewell, C. *Acta Crystallogr., Sect. C: Cryst. Struct. Commun.* **2007**, *63*, 440–444.

[56] Mootz, D.; Albert, A.; Schaefgen, S.; Staeben, D. *J. Am. Chem. Soc.* **1994**, *116*, 12045–12046.

[57] Glendening, E. D.; Feller, D. *J. Am. Chem. Soc.* **1996**, *118*, 6052–6059.

[58] Xenides, D.; Randolf, B. R.; Rode, B. M. *J. Chem. Phys.* **2005**, *122*, 174506.

[59] Andrade, S.; Gonçalves, L.; Jorge, F. E. *J. Mol. Struct.: THEOCHEM* **2008**, *864*, 20–25.

[60] Ozutsumi, K.; Natsuhara, M.; Ohtaki, H. *Bull. Chem. Soc. Jpn* **1989**, *62*, 2807–2818.

[61] Fukuhara, K.; Ikeda, K.; Matsuura, H. *J. Mol. Struct.* **1990**, *224*, 203–224.

[62] Boucher, L.; Katz, J. *J. Am. Chem. Soc.* **1967**, *89*, 1340–1345.